PLANT SCIENCE TODAY
ISSN 2348-1900 (online)
Vol 11(sp4): 01–11
https://doi.org/10.14719/pst.5810

HORIZON
e-Publishing Group
HePG

RESEARCH ARTICLE

Characterization of biochar produced from paperboard sludge: A sustainable approach for waste management and resource recovery

Vaishnavi P[1], Sherene Jenita Rajammal T[1*], Baskar M[1], Vanniarajan C[2], Ramjani SA[3], Senthil K[1] & Selvamurugan M[4]

[1]Department of Soil Science and Agricultural Chemistry, Anbil Dharmalingam Agricultural College and Research Institute, Tamil Nadu Agricultural University, Coimbatore 641 003, Tamil Nadu, India

[2]Department of Genetics and Plant Breeding, Anbil Dharmalingam Agricultural College and Research Institute, Tamil Nadu Agricultural University, Coimbatore 641 003, Tamil Nadu, India

[3]Department of Renewable Energy Engineering, Agricultural Engineering College and Research Institute, Tamil Nadu Agricultural University, Coimbatore 641 003, Tamil Nadu, India

[4]Environmental Science, Horticultural College and Research Institute (Women's), Tiruchirappalli, Tamil Nadu Agricultural University, Coimbatore 641 003, Tamil Nadu, India

*Email: shereneraj@yahoo.co.in

OPEN ACCESS

ARTICLE HISTORY
Received: 14 October 2024
Accepted: 11 November 2024
Available online
Version 1.0 : 25 December 2024
Version 2.0: 27 August 2025

Check for updates

Additional information
Peer review: Publisher thanks Sectional Editor and the other anonymous reviewers for their contribution to the peer review of this work.

Reprints & permissions information is available at https://horizonepublishing.com/journals/index.php/PST/open_access_policy

Publisher's Note: Horizon e-Publishing Group remains neutral with regard to jurisdictional claims in published maps and institutional affiliations.

Indexing: Plant Science Today, published by Horizon e-Publishing Group, is covered by Scopus, Web of Science, BIOSIS Previews, Clarivate Analytics, NAAS, UGC Care, etc
See https://horizonepublishing.com/journals/index.php/PST/indexing_abstracting

CITE THIS ARTICLE
Vaishnavi P, Sherene JRT, Baskar M, Vanniarajan C, Ramjani SA, Senthil K, Selvamurugan M. Characterization of biochar produced from paperboard sludge: A sustainable approach for waste management and resource recovery. Plant Science Today.2024;11(sp4):01-11. https:/doi.org/10.14719/pst.5810

Abstract

The pulp and paperboard industry are a significant industrial sector that consumes large quantities of fresh water and generates substantial volumes of wastewater. Treating this wastewater produces a considerable amount of sludge, which poses serious environmental challenges. This study proposes a sustainable solution by converting paperboard sludge (PBS) into biochar through slow pyrolysis at temperatures ≤500°C, offering an alternative approach to waste management and resource conservation. The physicochemical analysis of paperboard sludge biochar (PBSB) revealed a neutral pH of 7.49, EC (electrical conductivity) of 0.09 dS m^{-1}, an OC (organic carbon) content of 38.12% and a calcium carbonate ($CaCO_3$) content of24.5%. Proximate analysis of PBSB revealed an increased fixed carbon content of 10.27 %, total organic carbon (TOC) of 7.13% and reduced volatile matter and moisture levels. Micronutrients viz., iron (Fe) (5.06 mg L^{-1}), manganese (Mn) (419.3 mg L^{-1}), copper (Cu) (26.3 mg L^{-1}) and zinc (Zn) (66.1 mg L^{-1}), were also observed in PBSB. Fourier Transform Infrared Spectroscopy (FTIR) analysis identified various carbon-containing functional groups, including C-Cl, C-N, C-C, H-C=O, C-H and -C≡C-H, indicating substantial chemical transformations during pyrolysis. Scanning Electron Microscopy with Energy Dispersive X-ray (SEM-EDX) analysis revealed that PBSB consists of fine particles with a coarse, fluffy, spongy, porous structure, making it ideal for water adsorption. Elemental analysis through x-ray diffraction (XRD) showed high carbon and oxygen content and significant amounts of aluminosilicates, carbonates and nutrients like phosphorus (P) and potassium (K), suggesting PBSB as a potential slow-release fertilizer. This research highlights the potential of biochar derived from paperboard waste as a sustainable solution for effective waste management and resource recovery.

Keywords

AAS; biochar production; FTIR; physicochemical analysis; proximate analysis; SEM-EDX; TOC; XRD

Introduction

In India, the pulp and paperboard industry are a significant consumer of water, with each tonne of paper production generating 72 to 225 cubic meters of wastewater, depending on the production method employed (1). Sustainable solutions for waste management, such as biochar production through methods like pyrolysis, gasification, hydrothermal carbonization (HTC), slow pyrolysis and fast pyrolysis, are being explored (2, 3). These methods reduce waste and produce biochar, which has environmental and agricultural applications, offering a dual benefit to waste management in the paper industry.

The large volumes of wastewater this industry generates must be treated to meet environmental quality standards before reusing. Effluent treatment in the pulp and paperboard industry generates a substantial amount of sludge, creating a significant environmental burden (4). One tonne of paper typically generates 40-50 kg of dry sludge (5). Landfill disposal is the predominant practice for managing this sludge (6). However, landfilling poses significant environmental risks, including leaching contaminants into groundwater and releasing greenhouse gases, exacerbating pollution and climate change concerns.

Given these challenges, implementing effective sludge management strategies is essential to mitigate the environmental burden (7). With increasingly stringent environmental regulations, waste management remains one of the primary challenges for the pulp and paperboard industry (1). Sustainable and efficient solutions must address both environmental and economic considerations. Historically, landfilling has been the primary method for sludge disposal, but the need for alternative approaches is now more pressing than ever (6).

Waste from the paperboard industry can be repurposed as raw material for various applications, underscoring the need to establish sustainable processes. Over the past two decades, researchers have explored innovative methods to transform this waste into valuable resources. Among the most notable approaches are carbon sequestration and soil amendment. In acidic soils, it serves as a liming material, neutralizing pH levels and creating a favorable environment for plant growth. Additionally, in loamy soils, it enhances water-holding capacity. Biochar, in particular, has been shown to increase soil OC content and stimulate carbon sequestration by suppressing organic matter turnover (8).

As reported by previous studies, PBS can also be utilized in dried formulations as agricultural fertilizers, building materials and insulation materials (6). Its high carbon content makes PBS a potential feedstock for producing activated carbon, which can be applied to soils to enhance carbon levels (9). This method enriches soil carbon and addresses environmental concerns related to waste disposal while conserving natural resources.

Increasing soil carbon content provides numerous environmental benefits aligned with sustainability goals. A key advantage is carbon sequestration, which suppresses the long-term turnover of soil organic matter. Enhanced soil carbon improves soil health by boosting nutrient retention, water-holding capacity, microbial activity and overall soil structure, increasing agricultural productivity. Furthermore, higher soil carbon aids water conservation by enabling soils to retain more moisture, reducing irrigation needs and improving aeration (10).

This study aims to address these challenges by exploring the uniformity of carbon-rich biochar derived from the pyrolysis of PBS. It evaluates the biochar's physical and chemical properties and examines how varying input components influence these properties to determine potential applications. Techniques such as Fourier Transform Infrared Spectroscopy (FTIR), SEM-EDX, XRD, proximate analysis, and comprehensive physicochemical analysis were employed to characterize both raw PBS and the resulting biochar.

Materials and Methods

Study area

The study area is in Mondipatti Village, Manaparai Taluk, Tiruchirappalli district, Tamil Nadu, at Tamil Nadu Newsprint and Paper Limited (TNPL) - Unit II. This facility utilizes waste paper and imported pulp as raw materials to manufacture multi-layer coated paper boards. Positioned at approximately 10° 41' N latitude and 78° 26' E longitude, the plant has an annual production capacity of around 200,000 tons. Additionally, it processes approximately 5,000 cubic meters of effluent daily through a state-of-the-art effluent treatment plant (ETP).

Sample collection

Paperboard sludge (PBS) was sourced from the ETP of TNPL Unit II in Mondipatti, Tiruchirappalli, Tamil Nadu. These solid wastes were generated as a by-product of the effluent treatment process. The raw PBS was collected in clean polyethylene bags and shade-dried for 3 to 5 days to reduce its moisture content effectively, preparing it for further analysis. The bags were properly sealed and stored in moisture-free areas to prevent contamination during sample collection to ensure sample integrity.

Biochar production

Pyrolysis is a widely used method for the thermal conversion of biomass. In this study, slow pyrolysis was employed to convert PBS into biochar. This process involves thermally treating biomass in an environment with limited or no oxygen (11). A pyrolyzer with a capacity of 10 kg was used for biochar production. Slow pyrolysis, characterized by a low heating rate of approximately 0.1-1°C per second, is known for yielding a higher proportion of char. During the slow pyrolysis of PBS, the biomass was heated to approximately 500°C for 1 to 4 hours.

This process effectively transformed the PBS into carbon-rich biochar, as Fig. 1 and 2 illustrated. After pyrolysis, the biochar was allowed to cool, ground into a fine powder and made suitable for various applications, including soil enhancement, water filtration and carbon sequestration (1).

Physicochemical analysis of PBS and PBSB

All physicochemical parameters were measured following standard procedures. The samples pH and EC were determined using a digital pH meter and conductivity meter with a solid-to-water suspension ratio of 1:2.5 (12). Organic carbon (OC) content was assessed using the Walkley-Black method (13). The total N, P, K, calcium (Ca^{2+}) and magnesium (Mg^{2+}) content in the samples were extracted using a mixture of perchloric acid ($HClO_4$), sulphuric acid (H_2SO_4) and HNO_3 (nitric acid). The $CaCO_3$ (calcium

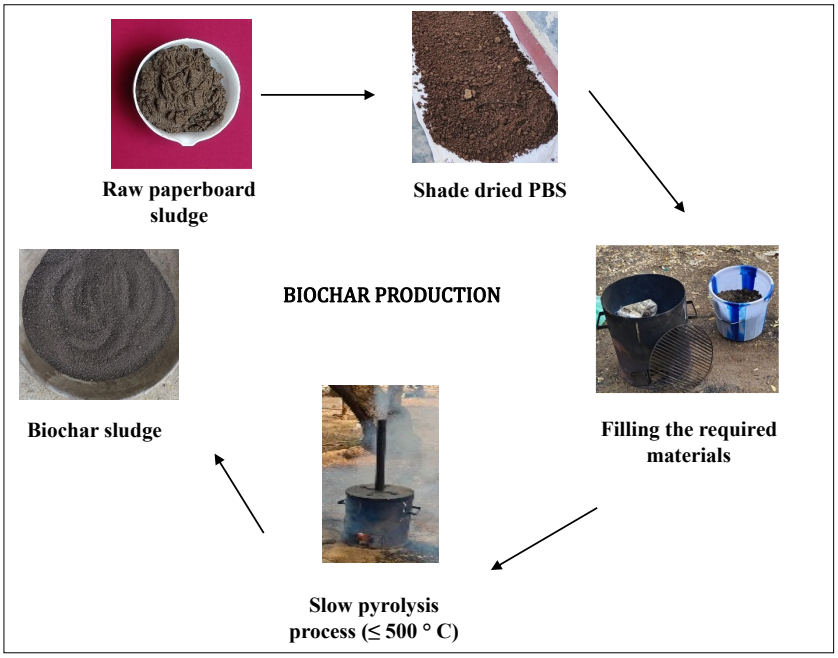

Fig. 1. Biochar production through a slow pyrolysis process.

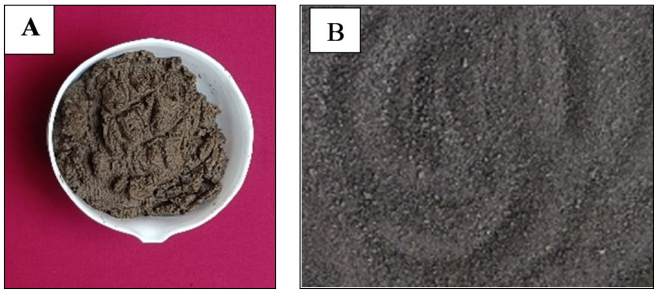

Fig. 2. Visual observation of (A) PBS and (B) PBSB.

carbonate) content was determined by treating the sample with HCl (hydrochloric acid) and measuring the volume of CO_2 (carbon dioxide) evolved. Micronutrients such as Cu, Fe, Mn and Zn were extracted using an acid digestion method and analyzed with an Atomic Absorption Spectrophotometer (Thermo Electron; Model IRIS Intrepid IIXDL, iCe 3000 series, USA) (14).

Proximate analysis for PBS and PBSB

Proximate analysis offers insights into the moisture content, volatile matter, ash content and fixed carbon content of PBS and PBSB, providing a comprehensive understanding of their composition.

Moisture content

The moisture content of PBS and PBSB samples was determined by heating the sample to a temperature slightly above the boiling point of water (105°C) for 8 hours. This process allows the water within the PBS and PBSB to evaporate, leading to a change in weight. Once the weight stabilizes, the difference between the initial and final weights is used to calculate the moisture content, expressed as a percentage of the sample. The formula for moisture content as shown in equation number (1) (15):

$$\text{Moisture content (\%)} = \frac{M_i - M_f}{M_i} \times 100 \qquad \text{(Eqn.1)}$$

Where M_i is the initial weight of moisture content, M_f is the final weight of moisture content.

Volatile matter

The volatile matter content of PBS and PBSB was determined using standard methods (14). A pre-weighed crucible containing a dried sample of PBS or PBSB was heated in a muffle furnace at 900°C for 1 hour in a non-oxidizing atmosphere. After heating, the crucible was cooled in a desiccator and weighed. This process was repeated in 30-minute intervals until a constant weight was achieved. The percentage of volatile matter was calculated using the following formula and was shown in equation number (2):

$$\text{Volatile matter (\%)} = \frac{M_f - V_f}{M_f} \times 100 \qquad \text{(Eqn. 2)}$$

Where M_f is the final weight of moisture content and V_f is the final weight of volatile matter

Ash content

To determine the ash content of PBS and PBSB, the dried samples were weighed with the crucible and then heated in a muffle furnace at 750°C for 1 hour. After heating, the crucible containing the ash was cooled in a desiccator and reweighed (15). The ash content percentage was calculated using the following formula and also shown in equation (3):

$$\text{Ash content (\%)} = \frac{W_{AF}}{M_f} \qquad \text{(Eqn. 3)}$$

Where W_{Af} is the final weight of ash content and M_f is the final weight of moisture content

Fixed carbon

The fixed carbon content of PBS and PBSB is calculated by subtracting the percentages of moisture content, ash content and volatile matter from the total composition. This relationship is represented by the following equation (15):

$$\text{Fixed carbon (\%)} = 100 - (\%MC + \%Ash + \%VM) \qquad \text{(Eqn. 4)}$$

Total organic carbon (TOC)

Dry the sample at 105°C until it reaches a constant weight. Weigh the dried sample and transfer it to a pre-weighed porcelain crucible. Heat the crucible containing the sample in a muffle furnace at 550-600°C for approximately 4 hours. After 4 hours, allow the crucible to cool and then weigh it. Calculate the weight loss by determining the difference between the initial and final weights of the crucible with the sample. This weight loss corresponds to the TOC content in the sample (1).

TOC (%) = (Weight loss upon ignition / initial weight of the sample) x 100 (Eqn. 5)

(Weight loss upon ignition = Initial weight of sample - Weight of crucible with residue after ignition)

Fourier transform infrared spectrometer (FT-IR)

FT-IR spectra were recorded using a Perkin Elmer Spectrum II Fourier Transform Infrared Spectrometer with KBr pellets. The sample was dried, powdered and sieved through a 2 mm sieve. A homogeneous mixture of PBS was prepared using a mortar and pestle before FT-IR analysis. The samples were placed directly into the holder and data were collected from 4000 cm^{-1} to 400 cm^{-1} using 21 CFR Part 11 software. Reference spectra were obtained before each sample analysis. Peak values were recorded and each analysis was repeated twice for confirmation (16).

Scanning electron microscope - energy dispersive x-ray spectroscopy (SEM – EDX)

For scanning electron microscopy (SEM), 10 mg of PBS and PBSB were placed on high-purity aluminum stubs and allowed to air dry at 37°C. Using a sputter coater, the samples were coated under a vacuum with approximately 25 nm of high-purity platinum. A specific area was selected for elemental analysis of PBS and PBSB and the sediment elements were analyzed using a high-resolution scanning electron microscope equipped with an EDAX system (14).

X-ray diffraction analyzer (XRD)

X-Ray Diffraction experiments were performed with a PANalytical empyrean diffractometer (PANalytical Expert TERP) equipped with a Cu-X ray source (k = 1.5404 Å), operated at 45Kv and 30mA. The prepared samples were placed on a quartz holder for analysis. Each diffractogram was measured at 2θ intervals of 0.05°, within the range of 5°-90° (4).

Results and Discussion

Physico-chemical properties of PBS and PBSB

Table 1 presents a comparative analysis of the physicochemical properties of PBS and PBSB. PBS's pH was slightly acidic at 6.84, whereas PBSB's pH was neutral at 7.49. PBS's EC was measured at 2.43 dS m^{-1}, compared to 0.90 dS m^{-1} for PBSB. These results are consistent with previous studies (9, 16-18).

The slightly acidic pH of PBS (6.84) can be attributed to its low $CaCO_3$ content, which is insufficient to neutralize the acidity present in the material. This relationship between reduced $CaCO_3$ levels and lower pH has been documented in prior research (14). On the other hand, PBSB's neutral pH of 7.49 results from its production at lower pyrolysis temperatures (≤500°C), resulting in neutral conditions. The shift towards neutral to alkaline pH in biochar is primarily due to the increased $CaCO_3$ content (17-20).

PBS displayed an OC content of 24.30%, lower than the 38.12% found in PBSB. The reduced OC in PBS can be attributed to its high cellulose fiber content (13, 21). The feedstock composition and pyrolysis conditions influence the OC content in biochar. During pyrolysis, OC primarily forms polyaromatic structures. It is noted that pyrolysis facilitates the development of aromatic rings that are resistant to microbial degradation, contributing to the enhanced stability of carbon in biochar (17).

Stable aromatic carbon is a significant factor in biochar's increased OC content (22, 23). Additionally, pyrolysis leads to the volatilization of organic compounds, with non-carbon elements such as oxygen and hydrogen being released. This process results in a higher concentration of carbon in the biochar. The reduction in mass of non-carbon components further stabilizes the carbon and elevates the OC content in biochar (24).

The C:N ratio of PBS was 13.9, while PBSB exhibited a higher ratio of 29.78, consistent with previous findings (9). The total N, P, K, Ca and Mg content in PBS were 1.74%, 0.58%, 0.84%, 4.39% and 2.36%, respectively, compared to PBSB, which contained 1.28%, 0.24%, 0.38%, 2.37% and 0.57%, respectively. These results align with other studies (9, 25). The higher Ca^{2+}, Mg^{2+}, and K levels in PBS compared to PBSB can be attributed to using virgin wood materials during paper production (14).

Virgin wood, a primary raw material for paperboard production, naturally contains significant amounts of Ca, Mg

Table 1. Physicochemical parameters of PBS and PBSB

S. No.	Parameters	Unit	PBS	PBSB
1	pH	-	6.84	7.49
2	EC	dS m^{-1}	2.43	0.09
3	Organic carbon	%	24.30	38.12
4	C: N ratio	-	13.96	29.78
5	CEC	C mol (p^+) kg^{-1}	2.50	5.00
6	$CaCO_3$	%	7.00	24.5
7	Total N	%	1.74	1.28
8	Total P	%	0.58	0.24
9	Total K	%	0.84	0.38
10	Total Ca	%	4.39	2.37
11	Total Mg	%	2.36	0.57
12	Zn	mg L^{-1}	95.82	66.08
13	Cu	mg L^{-1}	32.16	26.34
14	Fe	mg L^{-1}	1607.92	5.06
15	Mn	mg L^{-1}	532.78	419.34

and K minerals. These minerals are not fully removed during the pulping process and accumulate in the sludge. Additionally, $CaCO_3$ and other mineral fillers, commonly used to enhance paper quality, contribute to the elevated mineral content in PBS. During the pyrolysis of PBS into PBSB, many of these elements volatilize or transform into gaseous forms, resulting in a notable decrease in their concentration in PBSB.

The $CaCO_3$ content in PBS was 7.00%, whereas PBSB exhibited a significantly higher level of 24.5%. The increase in $CaCO_3$ in PBSB can be attributed to the removal of inorganic fillers from recycled paper during pyrolysis (13). The CEC of PBS was lower, at 2.5 C mol (p^+) kg^{-1}, compared to 5.00 C mol (p^+) kg^{-1} in PBSB. The CEC depends on the organic matter and clay content (25). The higher CEC of biochar reflects its greater ability to retain exchangeable cations through sorption pathways (26).

The micronutrient composition also showed significant differences between PBS and PBSB. PBS contained 95.82 mg L^{-1} of Zn, 32.16 mg L^{-1} of Cu, 1607.92 mg L^{-1} of Fe and 532.78 mg L^{-1} of Mn. In contrast, PBSB contained 66.08 mg L^{-1} of Zn, 26.34 mg L^{-1} of Cu, 5.06 mg L^{-1} of Fe and 419.34 mg L^{-1} of Mn.

Proximate analysis for PBS and PBSB

The proximate analysis of PBS and PBSB, as shown in Table 2, reveals significant differences in their composition. The moisture content of PBS was recorded at 50.6%, while PBSB exhibited a much lower moisture content of 0.55%. The ash content in PBSB was significantly higher at 78.29%, compared to 18.01% in PBS. The findings align with previously performed investigations (18, 20).

The volatile matter in PBS was 28.9%, whereas PBSB had a lower volatile matter content of 10.89%. This difference can be attributed to variations in the organic matter content between PBS and PBSB (14). Additionally, for PBSB, the volatile matter content is influenced by the pyrolysis temperature (27).

The fixed carbon content was 2.49% in PBS and increased to 10.27% in PBSB, highlighting the effect of pyrolysis in converting PBS into a carbon-rich material. This transformation makes PBSB suitable for applications such as soil enhancement, water filtration and carbon sequestration. The TOC of PBS was 1.03%, while PBSB demonstrated a significantly higher TOC of 7.13%, which aligns with a previous study (1).

Functional groups identified for PBS and PBSB

The functional groups in PBS and PBSB, as shown in Table 3, reveal diverse chemical compositions. In PBS, the identified functional groups include =C-H (methine group), C-C (alkene group), N-H (primary amine group), C=O (carbonyl group), H-C=O (carboxyl group) and C-H (Fig. 3). A broad band at 870 cm^{-1} in PBS may indicate the presence of $CaCO_3$ and corresponds to significant C-H stretching in aromatic groups. The absorption of C-H bond in PBS may be due to the mulling oil used in paper production. The peak at 995.53 cm^{-1} may be attributed to the bending vibrations of methylene or alkene groups =C-H with strong intensity. These =C-H methine or alkene groups, representing alkenes or unsaturated hydrocarbons, could arise from the breakdown of resin acids, unsaturated fatty acids, or other organic compounds in the wood or recycled fibers used in paperboard production (26). The peak at 1406.27 cm^{-1} may correspond to C-C stretching in medium-intensity aromatic groups. A broadband at 1628.41 cm^{-1} may be associated with the N-H bending vibrations of primary amines (asymmetric stretching), suggesting a partial breakdown of nitrogenous compounds. This breakdown may lead to amide or amine functional groups forming in PBS, which enhance its nutrient content, making it more suitable for applications such as soil amendment or fertilizer (28).

Table 2. Proximate analyses and TOC for PBS and PBSB

S. No.	Parameter	Unit	PBS	PBSB
1	Moisture	%	50.60	0.55
2	Ash	%	18.01	78.29
3	Volatile matter	%	28.90	10.89
4	Fixed carbon	%	2.49	10.27
5	Total organic carbon (TOC)	%	1.03	7.13

Table 3. Summary of identified FTIR band observed in PBS and PBSB

PBS				PBSB			
Peak value (cm^{-1})	Nature of band stretching (cm^{-1})	Functional group	Intensity	Peak value (cm^{-1})	Nature of band stretching (cm^{-1})	Functional group	Intensity
870	C-H bend	Aromatics	Strong	850	C-Cl Stretching	Alkyl halides	Medium
995.53	(= C – H) bend	Methylene group or Alkenes group	Strong	873.28	C-H Stretching	Aromatics group	Strong
1406.27	(C–C) Stretching (ring)	Aromatics group	Medium	1031.37	C – N Stretching	Aliphatic amines	Medium
1628.41	N – H bend	1° amines (asymmetric)	Medium	1416.58	C – C Stretching	Aromatics group	Medium
1779.94	C = O Stretching	Anhydrides group **	Strong	2813.81	H – C = O: C- H Stretching (or) -COOH	Aldehydes group (or) Carbonyl group	Medium
2794.01	H – C = O: C-H Stretching	Aldehydes group	Medium	2882.99	C – H Stretching	Alkanes group	Medium
2882.67	C -H Stretching	Alkanes	Medium	3276.95	- C ≡ C – H: C- H Stretching (or) O-H stretching	Alkynes (terminal) group or Alcohols groups**	(n- Narrow, s - Sharp) or (br-Broad, s-Sharp)
3364.48	N-H Stretching	1°, 2° amines and amides	Medium	-	-	-	-

Anhydrides group ** - due to the C - O stretch it absorbs in the fingerprint region

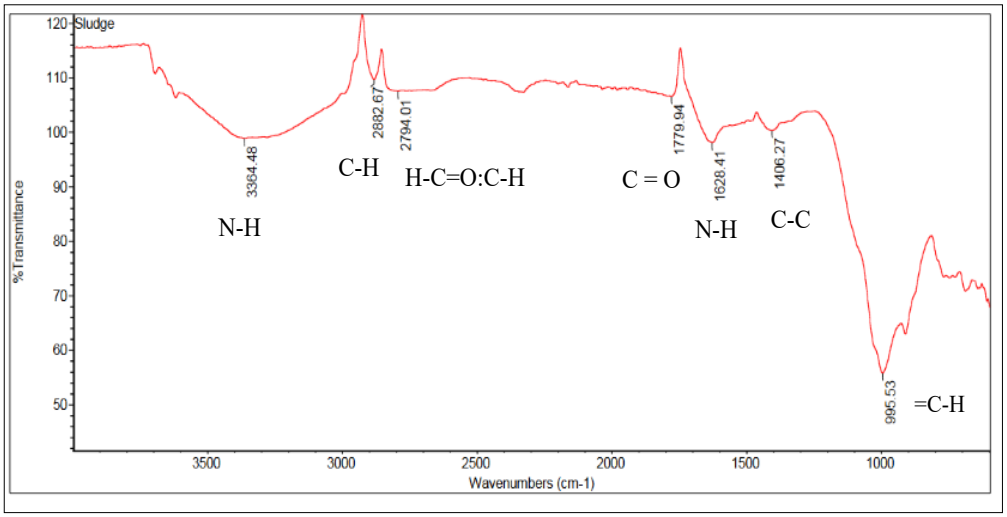

Fig. 3. FT-IR analysis reveals the presence of various functional groups in PBS, including (=C-H, C-C, N-H, C=O, H-C=O and C-H).

The peak at 1779.94 cm^{-1} corresponds to C=O (carbonyl group) stretching in anhydrides, potentially formed through the oxidation of organic materials during the papermaking process (4). A medium-intensity peak at 2794.01 cm^{-1} can be attributed to C-H stretching in aldehyde groups, related explicitly to carbonyl stretching of H-C=O. Meanwhile, the peak at 2882.67 cm^{-1} is linked to C-H stretching, suggesting the presence of saturated hydrocarbons (alkanes). The C-H absorptions in PBS are likely due to mulling oil, commonly employed in the paperboard industry to enhance coating quality, pigment mixing and ink absorption for better print results.

Lastly, the broad band at 3364.48 cm^{-1} corresponds to N -H stretching in primary and secondary amines and amides, indicating N-containing functional groups in the PBS.

The main surface functional groups identified in biochar include hydroxyl, methyl, carboxylic and alkene groups (28). Biochar pyrolyzed at lower temperatures (200-400°C) contains a high concentration of oxygen-containing functional groups such as (-COOH, -OH, C=O and -CHO), which stimulate nutrient exchange and improve soil fertility (29, 30). In PBSB, the observed functional groups include C-Cl (halo or chloro group), C-N, C-C (aromatic group), H-C=O: C-H (aldehyde group) or -COOH or C=O (carbonyl group), C-H and -C≡C-H: C-H (alkene group) or O-H (alcohol group) (Fig. 4).

The broad band at 850 cm^{-1} in PBSB may correspond to C-Cl of alkyl halides with medium intensity, enhancing the biochar's ability to adsorb and retain organic pollutants. During the impregnation process, $CaCO_3$ might transform into calcium chloride or other C-Cl groups (31). A sharp peak at 873.28 cm^{-1} and another at 710 cm^{-1} are associated with C-H stretching in aromatic groups with strong intensity, indicating out-of-plane and in-plane bending vibrations of the carbonate ion. This may result from cellulose, hemicellulose and lignin decomposition during pyrolysis at relatively low temperatures (≤500 °C).

A peak at 1031.37 cm^{-1} may correspond to C-N stretching in aliphatic amines formed from nitrogenous biomass components during pyrolysis. These components may shift from the amine or amide group, improving the biochar's CEC and enhancing nutrient retention (32). The peak at 1416.58 cm^{-1} indicates C-C stretching in aromatic groups, representing a more graphitic and stable structure. This structural stability is crucial for long-term carbon sequestration.

A strong absorption band near 1440 cm^{-1} and another at 850 cm^{-1} suggests the presence of $CaCO_3$, with the band at 1440 cm^{-1} corresponding to asymmetric stretching of the carbonate

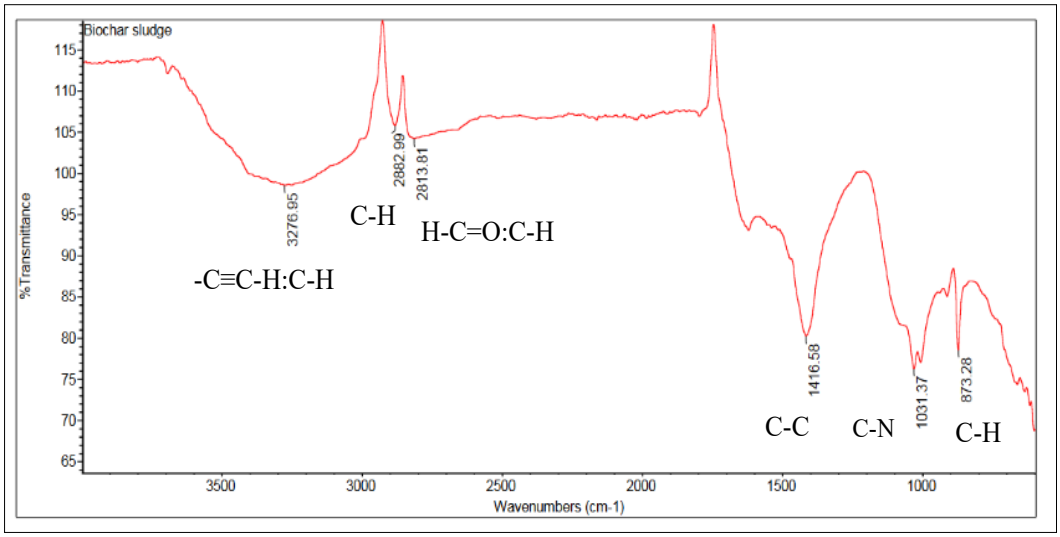

Fig. 4. FT-IR analysis reveals the presence of various functional groups in PBSB, including (C-Cl, C-N, C-C, H-C=O: C-H or -COOH or C=O, C-H, and -C≡C-H: C-H or O-H).

ion. The broadband at 2813.81 cm^{-1} may correspond to H-C=O: C-H stretching in the aldehydes group with medium intensity or -COOH or C=O of the carbonyl group. Meanwhile, the 2882.99 cm^{-1} band corresponds to C-H stretching in the alkanes group. The band at 3276.95 cm^{-1} may indicate -C≡C-H: C-H stretching in the alkynes group, which may form under low-oxygen conditions and suggest unsaturated carbon structures. All the functional groups observed in PBSB are influenced by its hydration state.

Scanning electron microscopy with energy-dispersive X-ray spectroscopy for PBS and PBSB (SEM-EDX)

The surface structures and morphology of PBS and PBSB were characterized using SEM, while their compositions were determined through EDX. SEM observations of PBS revealed a rough, wrinkled and flaky texture with a porous structure and a heterogeneous distribution of particles (Fig. 5). These features enable the sludge to effectively adsorb metals and various complex organic ions. The adsorption mechanism for metal and other complex ions on soil likely involves both physical and chemical adsorption at surface sites (33).

In contrast, the SEM micrograph of PBSB showed reduced particle size, a coarse surface, small cavities, holes and a mesoporous and microporous structure. Moreover, the surface of PBSB exhibited dispersion particles in the form of fluffy sponges and spherical-shaped fragments with deeper levels of fragmentation (16). The fluffy, spongy texture of PBSB can be attributed to its carbon matrix. Combined with the interconnected pores and voids within the biochar, this structure provides a large surface area crucial for water, nutrients, or pollutant adsorption. Due to the low pyrolysis temperature, PBSB may exhibit hydrophobic properties (Fig. 6).

The pores within biochar play a crucial role in facilitating solid-liquid interactions, enabling the passage of pollutants, nutrients, water, or electrolytes into the smaller pores within its internal structure (34, 35). Biochar's fluffy and spongy texture enhances its ability to improve soil aeration and water retention (36). Moreover, biochar produced at lower temperatures tends to be more hydrophobic, contributing to its greater structural strength than biochar produced at higher temperatures (37).

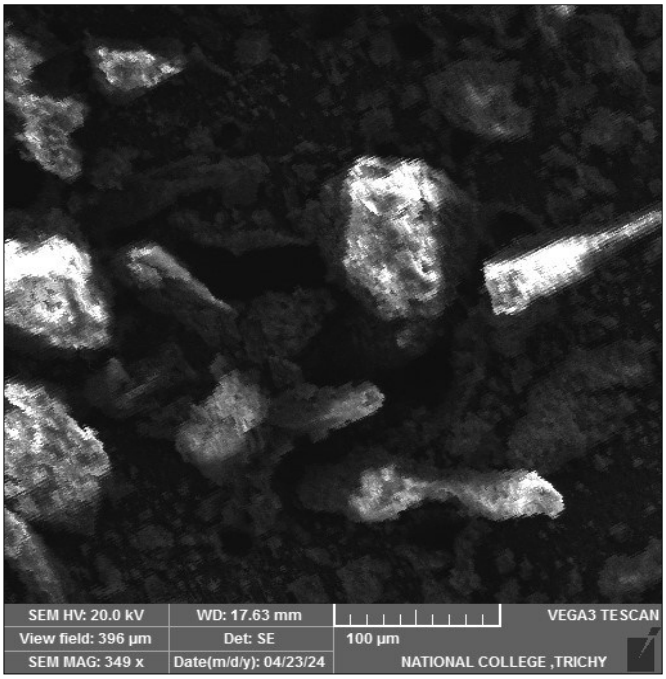

Fig. 5. SEM images of PBS at (349 x magnification) reveal a rough, wrinkled and flaky texture and a porous structure.

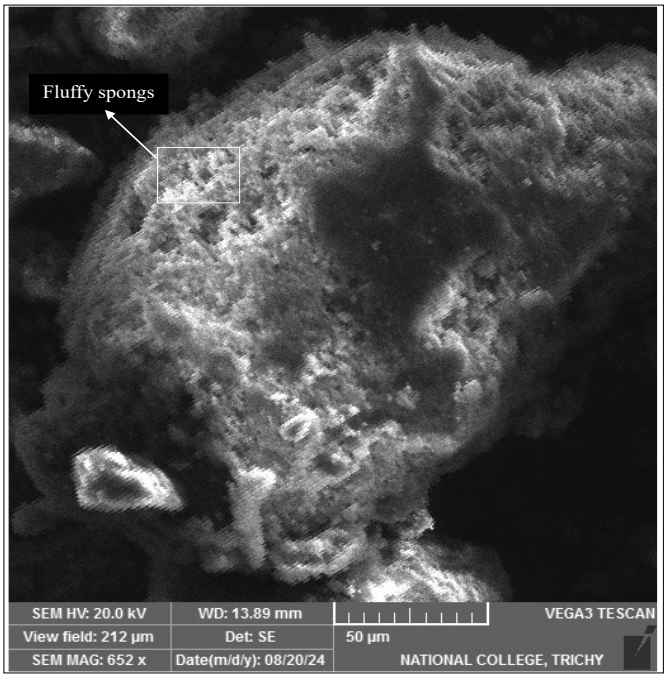

Fig. 6. SEM images of PBSB at (652 x magnification) reveal coarse, small cavities, holes, fluffy, spongy texture and a mesoporous structure.

Table 4. Elemental analysis of PBS and PBSB collected from Tamil Nadu Paper Limited (TNPL)

PBS			PBSB		
Element	**Weight %**	**Atomic %**	**Element**	**Weight %**	**Atomic %**
C – K	46.16	56.46	C K	34.46	45.43
O – K	41.53	38.14	O K	45.42	44.95
Na – K	0.42	0.27	Na K	0.33	0.23
Mg – K	0.43	0.26	Mg K	0.41	0.26
Al – K	1.43	0.78	Al K	3.70	2.17
Si – K	2.26	1.18	Si K	3.12	1.76
P – K	0.21	0.10	P K	1.31	0.67
S – K	0.88	0.40	S K	1.42	0.70
Cl – K	0.26	0.11	Cl K	0.38	0.17
K – K	0.24	0.09	K K	0.18	0.07
Ca – K	5.62	2.06	Ca K	8.45	3.34
Fe – K	0.56	0.15	Ti K	0.12	0.04
			Mn K	0.41	0.12
			Fe K	0.30	0.09
Totals	**100.00**		**Totals**	**100.00**	

The K and L following every element indicates the K and L shells of the specific atom

The EDX spectrum of PBS is shown in Table 4. Other elements detected in PBS include Ca (5.62% by weight), silicon (2.26% by weight) and aluminum (1.43% by weight), along with various trace elements. The presence of silicon and aluminum suggests the presence of aluminosilicate minerals, such as kaolinite ($Al_2Si_2O_5(OH)_4$), which are major components of clay minerals. These minerals contribute to soil's structural integrity and CEC. The individual weight percentages of the trace elements in PBS are also detailed in Table 4.

The EDX spectrum of PBSB is presented in Table 4. The predominant elements in PBSB were carbon (34.46% by weight) and oxygen (45.42% by weight). Silicon (3.12% by weight), aluminum (3.70% by weight) and Ca (8.45% by weight) were also present. These elements are commonly associated with aluminosilicates and carbonates. Silicon and aluminum in biochar indicate the presence of aluminosilicate minerals, such as kaolinite, which are crucial for preserving structural integrity and CEC in both soil and biochar (38).

Additionally, the P and K in biochar are slowly released into the soil, improving nutrient availability (24). The Ca in the form of $CaCO_3$ plays a crucial role in regulating soil pH. Calcium carbonate in biochar can significantly enhance long-term pH regulation in soils, making it more suitable for crop applications. $CaCO_3$ acts as a liming agent, neutralizing acidic soils by reacting with hydrogen ions to form calcium ions (Ca^{2+}) and carbonic acid (H_2CO_3). This H_2CO_3 can further dissociate into water (H_2O) and CO_2, reducing the concentration of hydrogen ions in the soil and raising the soil pH. This neutralization process improves the availability of essential nutrients that may otherwise be locked in acidic conditions, enhancing plant growth and crop productivity (8, 39). Fe (0.30%) and Mn (0.41%) are redox-sensitive elements that play a key role in redox reactions within the soil, undergoing oxidation and potentially triggering permeability transition pores (PTP). P (1.31%) and K (0.18%) by weight are essential nutrients in the soil and may enhance the value of PBSB as a slow-release fertilizer. Fig. 7 shows the XRD crystalline and amorphous phases of PBS and PBSB.

X-ray diffraction (XRD)

The crystalline and amorphous peak patterns of PBS and PBSB are shown in Table 5. XRD analysis was conducted to assess the properties of PBS (Fig. 8). PBS exhibited distinct peaks corresponding to its more crystalline phase. The strong crystalline peak at 29.6301° 2θ is attributed to calcite, aligning with the Ca utilized in paper manufacturing. Calcite is commonly used in the papermaking process to enhance the brightness and opacity of paper (40). The diffraction peaks at 44.66° 2θ and 64.84° 2θ are associated with periclase. The diffraction peaks at 11.7389° 2θ, 20.7562° 2θ and 31.20° 2θ suggest the presence of gypsum, a common by-product in paperboard production, particularly in processes that use calcium sulfate. The presence of gypsum in PBS is anticipated owing to the use of sulfur-containing chemicals in the pulping and bleaching procedures (41). Birnessite and cristobalite were

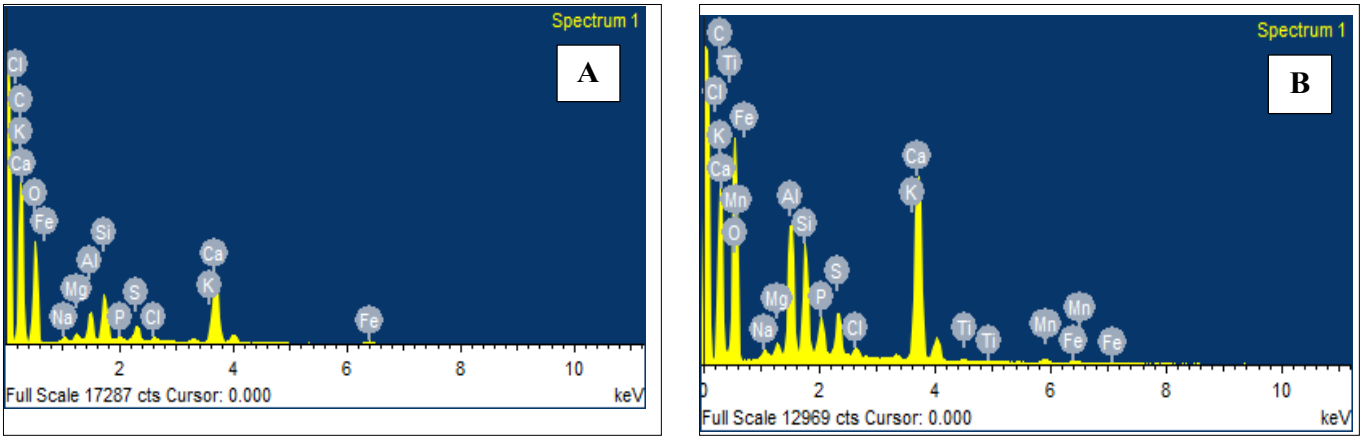

Fig. 7. EDX spectrum reveals the predominately occurred elements of (A) PBS and (B) PBSB.

Table 5. XRD analysis of PBS and PBSB

Visible	Reference code	Score	Compound name	Displacement (°2θ)	Scale factor	Chemical formula	Reference code	Score	Compound name	Displacement (°2θ)	Scale factor	Chemical formula
1	96-901-6707	81	Calcite	0.000	1.011	Ca6.00 C6.00 O18.00	96-900-1298	53	Calcite	0.000	0.883	Ca5.62 Mg0.38 C6.00 O18.00
2	96-202-1018	37	Digold indium palladium	0.000	0.156	Pd1.37 Au1.77 In0.86	96-901-3220	41	Periclase	0.000	0.140	Mg4.00 O4.00
3	96-901-1683	27	Bromargyrite	0.000	0.060	Ag4.00 Br4.00	96-900-1753	36	Gypsum (deuterated)	0.000	0.152	Ca8.00 S8.00 O24.00 D16.00
4	96-900-4468	28	Richetite	0.000	0.048	U36.00 Pb8.74 Fe0.47 Mg0.83 O173.00	96-900-1273	24	Birnessite	0.000	0.079	Mn2.00 O5.40 K0.46
5	96-900-1754	21	Gypsum (deuterated)	0.000	0.096	Ca8.00 S8.00 O24.00 D16.00	96-900-8229	8	Cristobalite	0.000	0.058	Si4.00 O8.00
6	96-500-0209	16	Cerussite	0.000	0.085	Pb4.00 C4.00 O12.00	96-900-9235	22	Kaolinite	0.000	0.074	Al2.00 Si2.00 O9.00 H4.00

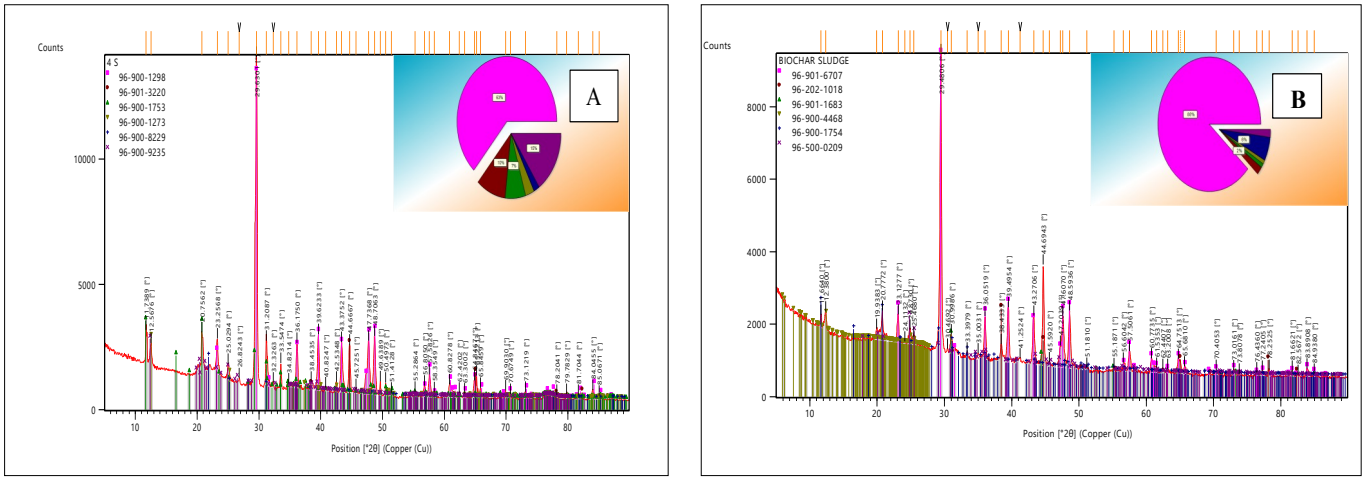

Fig. 8. XRD patterns reveal the crystalline and amorphous phases of (A) PBS and (B) PBSB.

also identified at 42.5348° 2θ and 31.2087° 2θ, respectively. Cristobalite likely formed during high-temperature processes or was present in raw materials containing silica, which is linked to using siliceous materials in paper production. The peak at 12.5676° 2θ indicates the presence of kaolinite, a common filler and coating material in the paper industry. Kaolinite contributed to the mineralogical composition of the sludge due to its abundance in raw materials and its stability during processing (42).

X-Ray Diffraction was performed to evaluate the PBSB properties (Fig. 8). PBSB exhibited distinct peaks of a more crystalline phase. The higher crystallinity may enhance the structural integrity of biochar, making it more resistant to microbial degradation and physical breakdown in the soil. This increased crystallinity helps biochar persist in the soil over the long term. The strong crystalline peaks observed at 29.4806° 2θ, 23.1277° 2θ and 39.4954° 2θ are attributed to the presence of calcite, indicating the presence of $CaCO_3$ used in paper production processes, which may serve as fillers or pigments (43, 44). During pyrolysis, calcite remains stable due to its resistance to low temperatures. Diffraction peaks observed at 38.433° 2θ, 44.6943° 2θ and 8.2525° 2θ indicate the presence of digold indium palladium. Additionally, bromargyrite and richetite were identified at the peaks of 30.9986° 2θ, 12.3800° 2θ and 24.1132° 2θ, respectively. The amorphous peaks observed at 6640° 2θ, 20.7772° 2θ, 51.1810° 2θ and 55.1871° 2θ correspond to gypsum (deuterated), while cerussite was identified at the peaks of 19.9383° 2θ, 24.8730° 2θ, 25.4680° 2θ, 35.0031° 2θ and 41.2524° 2θ.

Conclusion

This study highlights the potential of converting PBS into biochar through slow pyrolysis, which significantly modifies its physicochemical properties. PBSB generally has high levels of OC, fixed carbon, TOC, carbonates and aluminosilicates, as confirmed by FTIR spectroscopy and SEM-EDX analyses. These findings emphasize the efficacy of slow pyrolysis in enhancing carbon content and refining the chemical composition of PBS, corroborated by XRD reports.

Biochar improves soil structure by increasing porosity and enhancing water retention capacity, which promotes better root growth and moisture availability. It also boosts nutrient retention and exchange, improving nutrient accessibility for plants. These enhancements increase agricultural productivity while promoting sustainable and eco-friendly management practices. Additionally, biochar shows considerable promise as an option for pollutant removal.

The sustainable development of biochar production is particularly evident when utilizing industrial waste. This approach transforms waste materials into valuable resources, reducing reliance on landfills and minimizing greenhouse gas emissions. By creating closed-loop systems, where by-products of one process serve as inputs for another, this strategy supports the principles of the circular economy. Such integration promotes innovation, resource efficiency and environmental sustainability while enhancing local economies, improving waste management and enabling energy recovery. The circular bio-economy addresses waste issues through these practices and supports the transition towards more sustainable agricultural and industrial systems.

Acknowledgements

The authors express their sincere gratitude to TNPL Unit – II for their generous support and the instrumental facilities provided by the COE-SSH and thanks to S.A. Ramjani, Associate Professor at the Agricultural Engineering College and Research Institute, Kumulur, TNAU, Coimbatore, for invaluable assistance for biochar production and guidance throughout the study.

Authors' contributions

VP, SJRT, BM, VC, RSA, SK and SM have made substantial contributions to the conception, design, analysis, and interpretation of data for the work. VP and SJRT have contributed to critically drafting and revising the manuscript for important intellectual content. All authors read and approved the final manuscript.

Compliance with ethical standards

Conflict of interest: Authors do not have any conflict of interests to declare.

Ethical issues: None

References

1. Jaria G, Silva CP, Ferreira CI, Otero M, Calisto V. Sludge from paper mill effluent treatment as raw material to produce carbon adsorbents: An alternative waste management strategy. J Environ Manag. 2017;188:203-11. https://doi.org/10.1016/j.jenvman.2016.12.004
2. Zhang Y, Chen P, Liu S, Peng P, Min M, Cheng Y, et al. Effects of feedstock characteristics on microwave-assisted pyrolysis–A review. Bioresour Technol. 2017;230:143-51. https://doi.org/10.1016/j.biortech.2017.01.046
3. Capodaglio A, Callegari A, Dondi D. Properties and beneficial uses of biochar from sewage sludge pyrolysis. In: 5th International Conference on Sustainable Solid Waste Management; 2017.
4. Tawalbeh M, Rajangam AS, Salameh T, Al-Othman A, Alkasrawi M. Characterization of paper mill sludge as a renewable feedstock for sustainable hydrogen and biofuels production. Int J Hydrogen Energy. 2021;46(6):4761-75. https://doi.org/10.1016/j.ijhydene.2020.02.166
5. Bajpai P. Management of pulp and paper mill waste. Springer; 2015. https://doi.org/10.1007/978-3-319-11788-1
6. Likon M, Trebše P. Recent advances in paper mill sludge management. In: Show KY, Guo X, editors. Industrial Waste. Intechopen; 2012. p. 73-90. https://doi.org/10.5772/37043
7. Reckamp JM, Garrido RA, Satrio JA. Selective pyrolysis of paper mill sludge by using pretreatment processes to enhance the quality of bio-oil and biochar products. Biomass Bioenergy. 2014;71:235-44. https://doi.org/10.1016/j.biombioe.2014.10.003
8. Taskin E, de Castro Bueno C, Allegretta I, Terzano R, Rosa AH, Loffredo E. Multianalytical characterization of biochar and hydrochar produced from waste biomasses for environmental and agricultural applications. Chemosphere. 2019;233:422-30. https://doi.org/10.1016/j.chemosphere.2019.05.204
9. Ferreira CI, Calisto V, Cuerda-Correa EM, Otero M, Nadais H, Esteves VI. Comparative valorisation of agricultural and industrial biowastes by combustion and pyrolysis. Bioresour Technol. 2016;218:918-25. https://doi.org/10.1016/j.biortech.2016.07.047
10. Schofield HK, Pettitt TR, Tappin AD, Rollinson GK, Fitzsimons MF. Biochar incorporation increased nitrogen and carbon retention in a waste-derived soil. Sci Total Environ. 2019;690:1228-36. https://doi.org/10.1016/j.scitotenv.2019.07.116
11. Manyà JJ. Pyrolysis for biochar purposes: A review to establish current knowledge gaps and research needs. Environ Sci Technol. 2012;46(15):7939-54. https://doi.org/10.1021/es301029g
12. Jackson M. Soil chemical analysis. Prentice Hall of India Pvt. Ltd, New Delhi, India; 1973.
13. Nelson DW, Sommers LE. Total carbon, organic carbonand organic matter. In: Page AL, editor. Methods of Soil Analysis: Part 2 Chemical and Microbiological Properties. American Society of Agronomy, Inc., Soil Science Society of America, Inc. 1982. p. 539-79. https://doi.org/10.2134/agronmonogr9.2.2ed.c29
14. Méndez A, Fidalgo JM, Guerrero F, Gascó G. Characterization and pyrolysis behaviour of different paper mill waste materials. J Anal Appl Pyrolysis. 2009;86(1):66-73. https://doi.org/10.1016/j.jaap.2009.04.004
15. Agrafioti E, Bouras G, Kalderis D, Diamadopoulos E. Biochar production by sewage sludge pyrolysis. J Anal Appl Pyrolysis. 2013;101:72-78. https://doi.org/10.1016/j.jaap.2013.02.010
16. Oumabady S, Sebastian SP, Kamaludeen SPB, Ramasamy M, Kalaiselvi P, Parameswari E. Preparation and characterization of optimized hydrochar from paper board mill sludge. Sci Rep. 2020;10(1):773. https://doi.org/10.1038/s41598-019-57163-7
17. Guo M. The 3R principles for applying biochar to improve soil health. Soil Syst. 2020;4(1):9. https://doi.org/10.3390/soilsystems4010009
18. Sabarish K, Sebastian SP, Maheswari M, Balasubramaniam P, Ejilane J. Production and characterization of paper board mill ETP sludge derived hydrochar. Int J Environ Clim Change. 2021;11(11):1-8. https://doi.org/10.9734/ijecc/2021/v11i1130511
19. Venkatesh G, Gopinath KA, Reddy KS, Reddy BS, Prabhakar M, Srinivasarao C, et al. Characterization of biochar derived from crop residues for soil amendment, carbon sequestration and energy use. Sustainability. 2022;14(4):2295. https://doi.org/10.3390/su14042295
20. Junior A, Guo M. Efficacy of sewage sludge derived biochar on enhancing soil health and crop productivity in strongly acidic soil. Front Soil Sci. 2023;3:1066547. https://doi.org/10.3389/fsoil.2023.1066547
21. Kambo HS, Dutta A. A comparative review of biochar and hydrochar in terms of production, physico-chemical properties and applications. Renew Sustain Energy Rev. 2015;45:359-78. https://doi.org/10.1016/j.rser.2015.01.050
22. Vikrant K, Kim KH, Ok YS, Tsang DC, Tsang YF, Giri BS, et al. Engineered/designer biochar for the removal of phosphate in water and wastewater. Sci Total Environ. 2018;616:1242-60. https://doi.org/10.1016/j.scitotenv.2017.10.193
23. Yaashikaa P, Kumar PS, Varjani S, Saravanan A. A critical review on the biochar production techniques, characterization, stability and applications for circular bioeconomy. Biotechnol Rep. 2020;28:e00570. https://doi.org/10.1016/j.btre.2020.e00570
24. Lehmann J, Joseph S. Biochar for environmental management: An introduction. In: Lehmann J, Joseph S, editors. Biochar for environmental management. Routledge. 2015; p. 1-13. https://doi.org/10.4324/9781003297673-1
25. Turner T, Wheeler R, Oliver IW. Evaluating land application of pulp and paper mill sludge: A review. J Environ Manag. 2022;317:115439. https://doi.org/10.1016/j.jenvman.2022.115439
26. Holladay JE, White JF, Bozell JJ, Johnson D. Top value added chemicals from biomass-volume II, results of screening for potential candidates from biorefinery lignin. Pacific Northwest National Laboratory (PNNL), Richland, WA (United States); 2007. https://doi.org/10.2172/921839
27. Hossain MK, Strezov V, Chan KY, Ziolkowski A, Nelson PF. Influence of pyrolysis temperature on production and nutrient properties of wastewater sludge biochar. J Environ Manag. 2011;92(1):223-28. https://doi.org/10.1016/j.jenvman.2010.09.008
28. Bolan NS, Kunhikrishnan A, Choppala GK, Thangarajan R, Chung JW. Stabilization of carbon in composts and biochars in relation to carbon sequestration and soil fertility. Sci Total Environ. 2012;424:264-70. https://doi.org/10.1016/j.scitotenv.2012.02.061
29. Mandal S, Pu S, Adhikari S, Ma H, Kim DH, Bai Y, et al. Progress and future prospects in biochar composites: Application and reflection in the soil environment. Crit Rev Environ Sci Technol. 2021;51(3):219-71. https://doi.org/10.1080/10643389.2020.1713030
30. Ralebitso-Senior TK, Orr C. Microbial ecology analysis of biochar-augmented soils: Setting the scene. In: Ralebitso-Senior TK, Orr C, editors. Biochar Application. Elsevier. 2016; p. 1-40. https://doi.org/10.1016/B978-0-12-803433-0.00001-1
31. Manoko MC, Chirwa EMN, Makgopa K. Structural elucidation of magnetic biochar derived from recycled paper waste sludge. Chem Eng Trans. 2021;89:193-98. https://doi.org/10.3303/CET2188032
32. Mohan D, Sarswat A, Ok YS, Pittman Jr CU. Organic and inorganic contaminants removal from water with biochar, a renewable, low cost and sustainable adsorbent–A critical review. Bioresour Technol. 2014;160:191-202. https://doi.org/10.1016/j.biortech.2014.01.120
33. Yadav S, Chandra R. Detection and assessment of the phytotoxicity of residual organic pollutants in sediment contaminated with pulp and paper mill effluent. Environ Monit Assess. 2018;190:581. https://doi.org/10.1007/s10661-018-6947-1
34. dos Reis SG, Bergna D, Tuomikoski S, Grimm A, Lima EC, Thyrel M, et al. Preparation and characterization of pulp and paper mill sludge-activated biochars using alkaline activation: A box–Behnken design approach. ACS Omega. 2022;7(36):32620-30. https://doi.org/10.1021/acsomega.2c04290

35. Lima RMAP, dos Reis GS, Thyrel M, Alcaraz-Espinoza JJ, Larsson SH, de Oliveira HP. Facile synthesis of sustainable biomass-derived porous biochars as promising electrode materials for high-performance supercapacitor applications. Nanomaterials. 2022;12 (5):866. https://doi.org/10.3390/nano12050866

36. Liang J, Chen Y, Cai M, Gan M, Zhu J. One-pot pyrolysis of metal-embedded biochar derived from invasive plant for efficient Cr (VI) removal. J Environ Chem Eng. 2021;9(4):105714. https://doi.org/10.1016/j.jece.2021.105714

37. Nartey OD, Zhao B. Biochar preparation, characterization and adsorptive capacity and its effect on bioavailability of contaminants: An overview. Adv Mater Sci Eng. 2014;2014:715398. https://doi.org/10.1155/2014/715398

38. Wang Y, Zhang K, Lu L, Xiao X, Chen B. Novel insights into effects of silicon-rich biochar (Sichar) amendment on cadmium uptake, translocation and accumulation in rice plants. Environ Pollut. 2020;265 (PtB):114772. https://doi.org/10.1016/j.envpol.2020.114772

39. Hossain MZ, Bahar MM, Sarkar B, Donne SW, Ok YS, Palansooriya KN, et al. Biochar and its importance on nutrient dynamics in soil and plant. Biochar. 2020;2:379-420. https://doi.org/10.1007/s42773-020-00065-z

40. dos Reis GS, Guy M, Mathieu M, Jebrane M, Lima EC, Thyrel M, et al. A comparative study of chemical treatment by $MgCl_2$, $ZnSO_4$, $ZnCl_2$ and KOH on physicochemical properties and acetaminophen adsorption performance of biobased porous materials from tree bark residues. Colloids Surf A: Physicochem Eng Asp. 2022;642:128626. https://doi.org/10.1016/j.colsurfa.2022.128626

41. Deepika, Samriti, Sharma G, Kaur H, Kumar S, Chadha P. Sustainable utilization of industrial sludge in the construction industry. In: Kumar V, Bhat SA, Verma P, Kumar S, editors. Recent trends in management and utilization of industrial sludge. Springer, Cham; 2024. p. 209:53. https://doi.org/10.1007/978-3-031-58456-5_8

42. Harmsen J, Naidu R. Bioavailability as a tool in site management. J Hazard Mater. 2013;261:840-46. https://doi.org/10.1016/j.jhazmat.2012.12.044

43. Zhao B, Zhang J. Tetracycline degradation by peroxydisulfate activated by waste pulp/paper mill sludge biochars derived at different pyrolysis temperature. Water. 2022;14(10):1583. https://doi.org/10.3390/w14101583

44. Liu Z, Hughes M, Tong Y, Zhou J, Kreutter W, Lopez HC, et al. Paper mill sludge biochar to enhance energy recovery from pyrolysis: A comprehensive evaluation and comparison. Energy. 2022;239(Pt A):121925. https://doi.org/10.1016/j.energy.2021.121925